



Getting the bond back together: The strategies are unveiled for an aromatic C-C *ipso*-substitution reaction. This process allows for the one-pot cleavage of Ar-C bonds (e.g., in alkyl and acyl

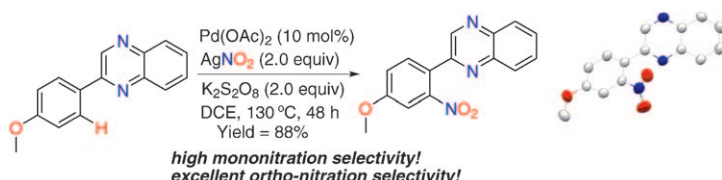
(hetero)aromatics, in benzonitriles, in α, α -disubstituted arylmethanols, and in carboxylic acids) for the formation of a new Ar-C bond (see picture).

Arylation Reactions

S. M. Bonesi,
M. Fagnoni* 13572–13589

The Aromatic Carbon–Carbon *ipso*-Substitution Reaction

COMMUNICATIONS



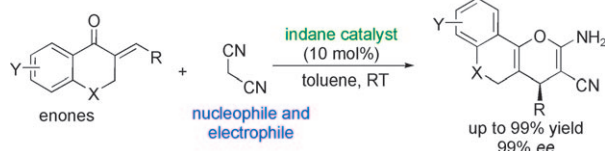
Nitration of N-heteroaromatics: The first example of palladium-catalyzed direct *ortho*-nitration of aryl C–H bonds is described. A range of azaaromatics, such as 2-arylquinoxalines, pyridines, pyrazoles, and *O*-methyl oximes, were nitrated with excellent chemo-

and regioselectivity (see scheme; DCE = 1,2-dichloroethane). Preliminary mechanistic investigations support a silver-mediated radical mechanism involving palladium(II/III) and/or palladium(II/IV) catalytic cycles under oxidizing conditions.

Regiospecific Nitration

Y.-K. Liu,* S.-J. Lou, D.-Q. Xu,
Z.-Y. Xu* 13590–13593

Regiospecific Synthesis of Nitroarenes by Palladium-Catalyzed Nitrogen-Donor-Directed Aromatic C–H Nitration



A surprising example of enantioselective cascade Michael–oxa–Michael–tautomerization reactions of malononitrile and benzylidenechromanones has been developed. In this case, malononitrile functions as both nucleophile and elec-

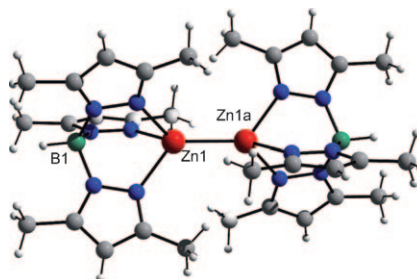
trophile. Meanwhile, a simple bifunctional indane amine–thiourea catalyst has been discovered to promote this process to afford high yields (up to 99%) and high to excellent enantiomeric excesses (81–99% *ee*).

Asymmetric Catalysis

Q. Ren, Y. Gao,
J. Wang* 13594–13598

Enantioselective Synthesis of Densely Functionalized Pyranochromenes via an Unpredictable Cascade Michael–Oxa–Michael–Tautomerization Sequence

Making it new! A novel synthetic pathway for the synthesis of Zn–Zn-bonded complexes (see graphic) under mild reaction conditions is presented.



Metal–Metal Interactions

S. Gondzik, D. Bläser, C. Wölper,
S. Schulz* 13599–13602

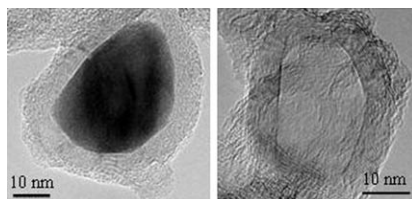
Novel Synthetic Pathway for New Zn–Zn-Bonded Compounds from Dizincocene

Carbon Nanocages

S. J. Teng, J. N. Wang,* B. Y. Xia,
X. X. Wang 13603–13608



A General Strategy for the Preparation of Hollow Carbon Nanocages by NH₄Cl-Assisted Low-Temperature Heat Treatment



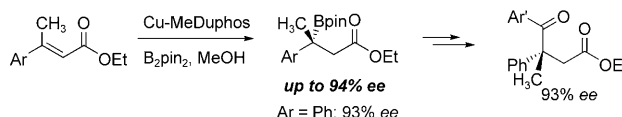
Empty cages: Iron/graphite core-shell nanoparticles are produced by pyrolysis of a mixture of acetylene and iron carbonyl. Then, the core-shell nanoparticles are heat treated in the range of 300–500 °C in the presence of NH₄Cl. After filtration in water, the trapped iron particles are completely removed and hollow carbon nanocages with a good graphitic structure are obtained (see graphic).

Asymmetric Synthesis

X. Feng, J. Yun* 13609–13612



Conjugate Boration of β,β -Disubstituted Unsaturated Esters: Asymmetric Synthesis of Functionalized Chiral Tertiary Organoboron Esters



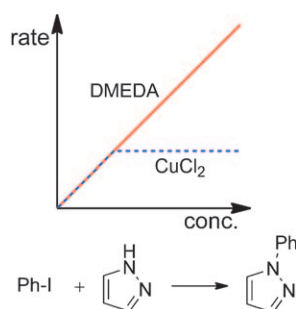
Challenging tertiary organoboron esters containing a β -ester group were prepared enantioselectively via the asymmetric conjugate boration of β,β -disubstituted α,β -unsaturated esters

with a copper-phosphine catalyst (see scheme). The functionalized organoboron derivatives can be utilized as a carbon nucleophile to form all-carbon quaternary centers.

Cross-Coupling Reactions

P.-F. Larsson, C. Bolm,
P.-O. Norrby* 13613–13616

Kinetic Investigation of a Ligand-Accelerated Sub-mol % Copper-Catalyzed C–N Cross-Coupling Reaction



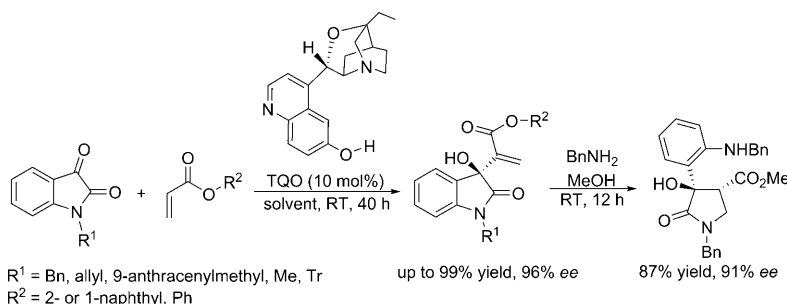
Unique ligand acceleration: A kinetic investigation of the copper-catalyzed C–N cross-coupling in the sub-mol % range reveals an exceptional ligand dependence. Dimethylethylenediamine (DMEDA) is unique in promoting this reaction, and even at a ratio of >2000:1 relative to the catalyst, the reaction order is still positive in DMEDA. This discovery allowed the development of milder reaction conditions. The reaction order in copper becomes zero at very low concentration.

Organocatalysis

X.-Y. Guan, Y. Wei,*
M. Shi* 13617–13621

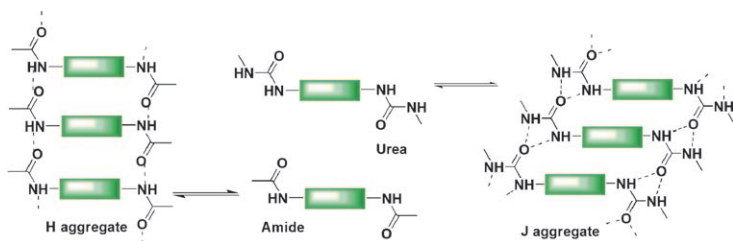


Construction of Chiral Quaternary Carbon through Morita–Baylis–Hillman Reaction: An Enantioselective Approach to 3-Substituted 3-Hydroxyoxindole Derivatives



A new enantioselective approach to obtain a tetrasubstituted chiral center at the C3 position of oxindoles via a catalytic asymmetric Morita–Baylis–Hillman reaction has been demonstrated. This reaction provides 3-substi-

tuted 3-hydroxy-2-oxindoles in good to excellent yields and *ee* values, which could be facily transformed to pharmaceutically more interesting compounds.



Gelled together: Self-assembly and gelation studies of bis-urea- and bis-amide-functionalised dialkoxynaphthalene chromophores (DAN-U and DAN-A, respectively) revealed contrasting J- and H-type aggregation

properties in solution, respectively (see scheme). DAN-U was found to be a “super-gelator” with much higher thermal stability, whereas DAN-A showed gelation with superior mechanical stability.

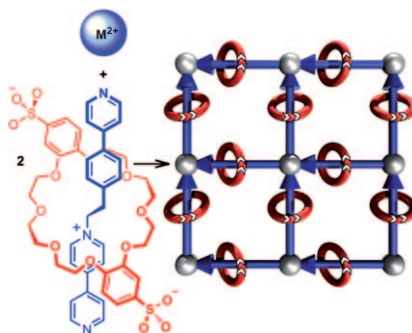
Gels

A. Das, S. Ghosh* 13622–13628

Contrasting Self-Assembly and Gelation Properties among Bis-urea- and Bis-amide-Functionalised Dialkoxynaphthalene (DAN) π Systems



Sometimes it's best to be neutral: The combination of a new, anionic [2]pseudorotaxane ligand and Zn^{II} ions results in the formation of neutral, ML_2 -style square grids. The layers can be pillared to create full three-periodic MOF structures that are neutral and porous. These materials represent the first examples of neutral porous MOFs in which one (or more) of the linkers is a mechanically interlocked molecule.



FULL PAPERS

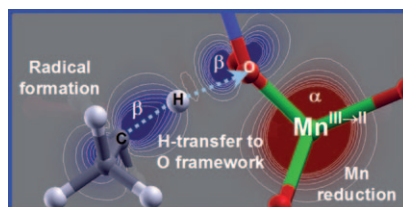
Supramolecular Chemistry

V. N. Vukotic,
S. J. Loeb* 13630–13637

One-, Two- and Three-Periodic Metal–Organic Rotaxane Frameworks (MORFs): Linking Cationic Transition-Metal Nodes with an Anionic Rotaxane Ligand



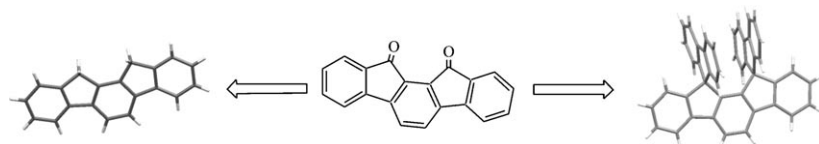
Radical propagation: The oxidation of hydrocarbons by Mn-doped nanoporous aluminophosphates takes place by an initial activation of the hydrocarbon molecule by means of a hydrogen transfer to the active site. This occurs through a homolytic cleavage of the C–H bond, in which the α -spin density is transferred to Mn, prompting its reduction, whilst the β -spin density is localised on the C atom, thus becoming a radical species, from which propagation reactions will take place.



Heterogeneous Catalysis

L. Gómez-Hortigüela,* F. Corà,
G. Sankar, C. M. Zicovich-Wilson,
C. R. A. Catlow 13638–13645

Catalytic Reaction Mechanism of Mn-Doped Nanoporous Aluminophosphates for the Aerobic Oxidation of Hydrocarbons



Two new blue/violet fluorophores based on the (2,1-*a*)-indeno[1,2-*b*]fluorenyl backbone have been prepared through original and efficient synthetic approaches. Their properties have

been compared with those of their corresponding positional isomers based on the (1,2-*b*)-indeno[1,2-*b*]fluorenyl backbone and those of related dispirofluorene heteroacenes.

Fluorophores

D. Thirion, C. Poriel,*
J. Rault-Berthelot, F. Barrière,
O. Jeannin 13646–13658

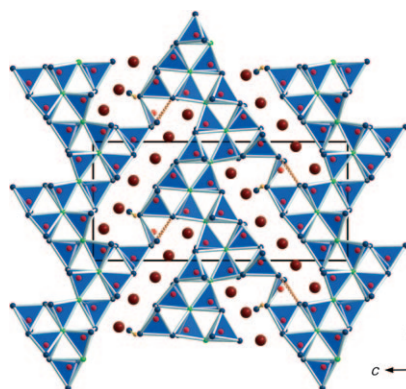
(2,1-*a*)-Indeno[1,2-*b*]fluorene Derivatives: Syntheses, X-ray Structures, Optical and Electrochemical Properties



Borate Crystals

S. C. Neumair, J. S. Knyrim,
O. Oeckler, R. Glaum, R. Kaindl,
R. Stalder, H. Huppertz* 13659–13670

Intermediate States on the Way to Edge-Sharing BO_4 Tetrahedra in $\text{M}_6\text{B}_{22}\text{O}_{39}\cdot\text{H}_2\text{O}$ ($\text{M}=\text{Fe}, \text{Co}$)

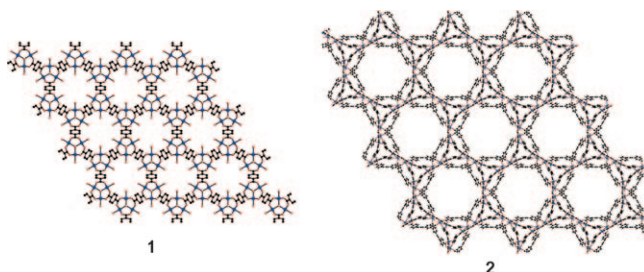


Having the edge: The new structure type of $\text{M}_6\text{B}_{22}\text{O}_{39}\cdot\text{H}_2\text{O}$ ($\text{M}=\text{Fe}, \text{Co}$) is built up from corner-sharing BO_4 tetrahedra, to form corrugated multiple layers interconnected by BO_3 groups. These BO_3 groups are distorted and close to BO_4 tetrahedra if additional oxygen atoms of the neighbouring tetrahedra are considered in the coordination sphere (see picture). This situation can be regarded as an intermediate state on the way to edge-sharing tetrahedra.

Metal–Organic Frameworks

I. A. Ibarra, X. Lin, S. Yang,
A. J. Blake, G. S. Walker, S. A. Barnett,
D. R. Allan, N. R. Champness,*
P. Hubberstey,
M. Schröder* 13671–13679

Structures and H_2 Adsorption Properties of Porous Scandium Metal–Organic Frameworks



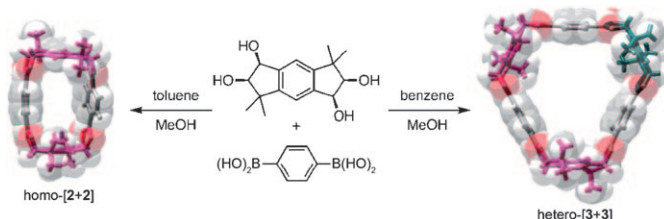
It's Sc^{III} andalous: $\{[\text{Sc}_3\text{O}(\text{L}^1)_3-(\text{H}_2\text{O})_3]\cdot\text{Cl}_{0.5}\text{OH}_{0.5}(\text{DMF})_4(\text{H}_2\text{O})_3\}_\infty$ (**1**) ($\text{H}_2\text{L}^1=1,4$ -benzenedicarboxylic acid) and $\{[\text{Sc}_3\text{O}(\text{L}^2)_2(\text{H}_2\text{O})_3]\text{OH}(\text{H}_2\text{O})_5-(\text{DMF})_\infty$ (**2**) ($\text{H}_3\text{L}^2=1,3,5$ -tris(4-carboxyphenyl)benzene) incorporate the trinuclear trigonal planar $[\text{Sc}_3(\text{O})-$

$(\text{O}_2\text{CR})_6]$ building block. After appropriate thermal treatment on the acetone-exchanged sample **2**, the generation of free metal coordination sites has been achieved to give an increase in the BET surface area in **2b**.

Boronic Esters

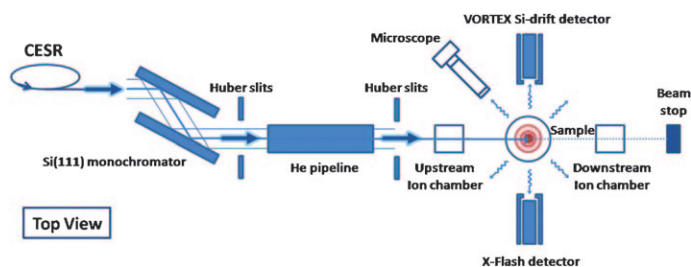
H. Takahagi,
N. Iwasawa* 13680–13688

Crystallization-Controlled Dynamic Self-Assembly and an On/Off Switch for Equilibration Using Boronic Ester Formation



Dynamic duo: Dynamic self-assembly of two macrocyclic boronic esters is achieved by reversible boronic ester formation (see figure). The reaction occurs by mixing diboronic acid and a

bis(1,2-diol) under neutral conditions and precipitation plays a key role in the selective formation of the two macrocycles. It is also possible to switch the equilibrium on and off.



Simple and effective investigation: The composition of ordered intermetallic nanoparticles (PtBi and PtPb) has been quantitatively studied by in situ X-ray fluorescence during active electrochemical control in solutions of sup-

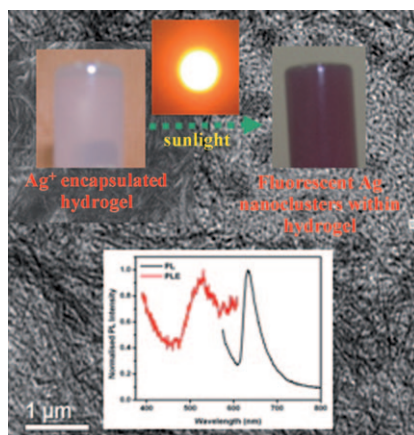
porting electrolyte and small organic molecules (see picture). This approach represents a simple, universal, nondestructive, and multifunctional method for the study of multi-element nanoparticles as electrocatalysts.

Electrocatalysts

*Y. Liu, M. A. Lowe, K. D. Finkelstein, D. S. Dale, F. J. DiSalvo, H. D. Abruna** 13689–13697

X-ray Fluorescence Investigation of Ordered Intermetallic Phases as Electrocatalysts towards the Oxidation of Small Organic Molecules

Silver nanoparticles: An N-terminally protected dipeptide-based hydrogel has been used to make fluorescent silver nanoclusters in the presence of sunlight at room temperature and at physiological pH by using a green chemistry approach. The fluorescent silver nanoclusters exhibit interesting fluorescence properties with a very narrow emission profile and large Stokes shift that may be useful in future applications.

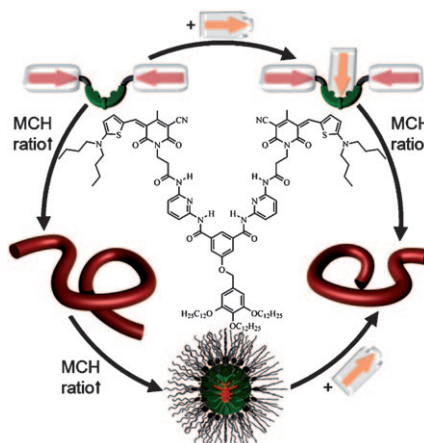


Fluorescent Nanoclusters

*B. Adhikari, A. Banerjee** 13698–13705

Short-Peptide-Based Hydrogel: A Template for the In Situ Synthesis of Fluorescent Silver Nanoclusters by Using Sunlight

The right direction: The directional character of orthogonal hydrogen-bonding and dipole–dipole interactions in conjugates of dipolar dyes and the Hamilton receptor (see figure) affords supramolecular polymers that are responsive to environmental changes and molecular stimuli.



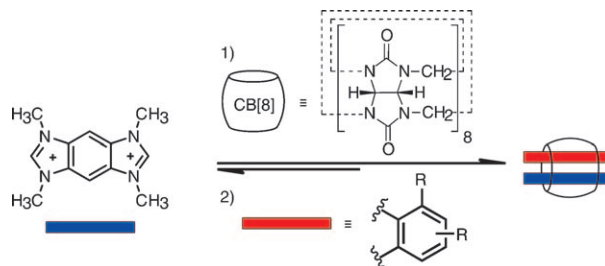
Self-Assembly

*R. Schmidt, S. Uemura, F. Würthner** 13706–13715

Solvent- and Guest-Responsive Self-Assembly of Hamilton Receptor Tethered Bis(merocyanine) Dyes

Self-Assembly

F. Biedermann, U. Rauwald,
M. Cziferszky, K. A. Williams,
L. D. Gann, B. Y. Guo, A. R. Urbach,*
C. W. Bielawski,*
O. A. Scherman* 13716–13722

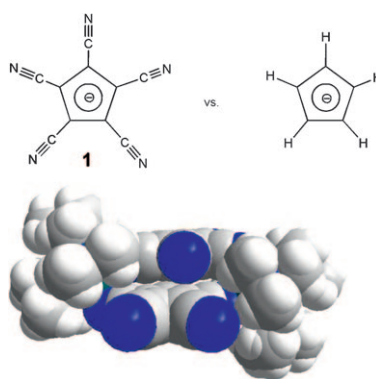


Aqueous sensing: Benzobis(imidazolium) (in blue)–cucurbit[8]uril complexes can bind and sense aromatic compounds (in red) in aqueous solution. Benzobis(imidazolium) (BBI) salts were used as new first guests for the macrocyclic host cucurbit[8]uril

(CB[8]). The aqueous binding behavior of BBI with CB[8] leads to a wide variety of ternary complexes and offers substantial advantages over viologens, including intrinsic fluorescence, higher chemical stability, and broader synthetic tunability.

Cyclopentadienide Chemistry

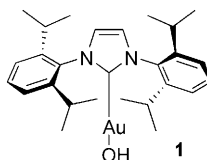
R. J. Less, M. McPartlin, J. M. Rawson,
P. T. Wood,*
D. S. Wright* 13723–13728



Easy does it: Deprotonation of $[\text{Et}_3\text{NH}][\text{C}_5(\text{CN})_5]$ with metal bases provides a very simple approach to coordination compounds containing the pentacyanocyclopentadienide anion, $[\text{C}_5(\text{CN})_5]^-$ (**1**). The absence of π bonding of the metal ions in the complexes $[\text{Na}(\text{thf})_{1.5}(\textbf{1})]_\infty$ and $[\{(\text{tmeda})_2\text{Na}(\textbf{1})\}_2]$ ($\text{tmeda} = \text{Me}_2\text{NCH}_2\text{CH}_2\text{NMe}_2$) results from dispersion of the negative charge from the C_5 -ring unit to the $\text{C}\equiv\text{N}$ groups, making the coordination chemistry of the $[\text{C}_5(\text{CN})_5]^-$ ion distinctly different from that of the cyclopentadienide ion.

Homogeneous Catalysis

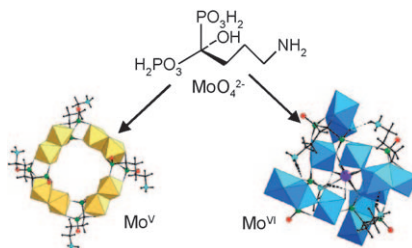
S. Gaillard,* J. Bosson, R. S. Ramón,
P. Nun, A. M. Z. Slawin,
S. P. Nolan* 13729–13740



[Au(OH)(IPr)] in catalysis: The use of a versatile $[\text{Au}(\text{OH})(\text{IPr})]$ complex (**1**) permits the in situ generation of the $[\text{Au}(\text{IPr})]^+$ ion by simple addition of a Brønsted acid. ^1H NMR studies of the in situ generation protocol reveal the formation of $[\text{Au}(\text{IPr})_2(\mu\text{-OH})][\text{BF}_4]$. This simple activation is tested in numerous reactions involving cationic gold(I) catalysis.

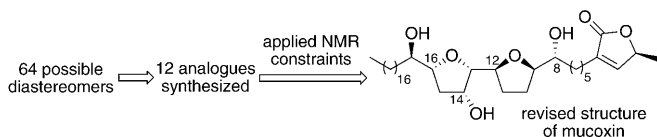
Polyoxometalates

J.-D. Compain, P. Mialane, J. Marrot,
F. Sécheresse, W. Zhu, E. Oldfield,*
A. Dolbecq* 13741–13748



POMs against cancer: The activity of hybrid organic–inorganic water-soluble cyclic polyoxometalates (POMs), which incorporate alendronate ligands, against three human tumor cell lines were investigated in vitro. The activity of the depicted Mo^{VI} complex is approximately four times better than the parent alendronate molecule.

Tetra- to Dodecanuclear Oxomolybdate Complexes with Functionalized Bisphosphonate Ligands: Activity in Killing Tumor Cells



Annonaceous acetogenins: Analysis of the NMR spectra of 12 stereoisomeric analogues of mucosin led to a number of structural constraints, limiting the

field of diastereomeric possibilities from 64 to 4. This led to the identification of the relative stereochemistry of mucosin.

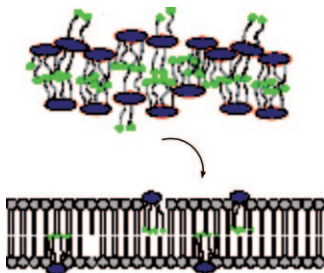
Structure Elucidation

J. Yan, A. Garzan, R. S. Narayan, C. Vasileiou,*
B. Borhan* 13749–13756

A Minimalist NMR Approach for the Structural Revision of Mucosin



Dansyl makes it better! Functionalisation of the tetraethylene glycol (TEG) tentacles of a cyclic phosphate-linked oligosaccharide (CyPLOS) macrocycle with dansyl residues resulted in high ion-transport activity and allowed deeper insight into the mechanism of action of this new class of artificial ionophores, with their strong tendencies to self-aggregate in aqueous solutions (see figure).

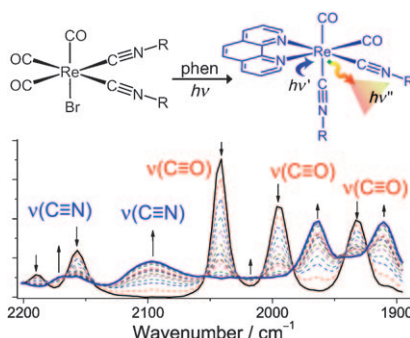


Synthetic Ion Transporters

C. Coppola, A. Paciello, G. Mangiapia, S. Licen, M. Boccalon, L. De Napoli, L. Paduano, P. Tecilla, D. Montesarchio* 13757–13772

Design, Synthesis and Characterisation of a Fluorescently Labelled CyPLOS Ionophore

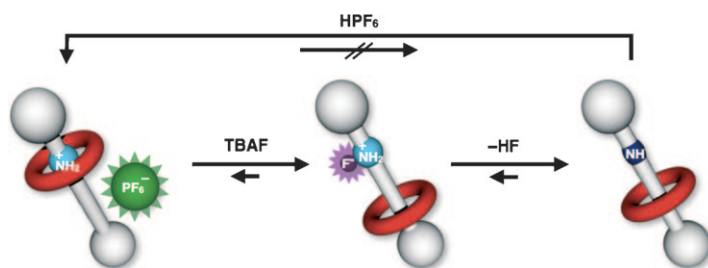
Tunable luminophore: A new class of rhenium(I) diimine luminophores, *cis,cis*-[Re(CO)₂(CNR)₂(N–N)]⁺ (R = 2,4,6-Cl₃C₆H₂, 4-ClC₆H₄, 4-Br-2,6-(CH₃)₂C₆H₂, 2,6-(CH₃)₂C₆H₃, 4-[(CH₃)₂N]C₆H₄, 4-(C₆H₅)C₆H₄, 4-*n*BuC₆H₄, *t*Bu), has been synthesized by a selective photochemical substitution reaction. This photosubstitution was studied by in situ IR spectroscopy (see picture; phen = phenanthroline). Most complexes display intense metal-to-ligand charge transfer phosphorescence with quantum yields of up to 0.37.



Rhenium Complexes

C.-C. Ko,* L. T.-L. Lo, C.-O. Ng, S.-M. Yiu 13773–13782

Photochemical Synthesis of Intensely Luminescent Isocyano Rhenium(I) Complexes with Readily Tunable Structural Features



Neutral and free: The neutralization of the ammonium group of crown ether/*sec*-ammonium salt-type rotaxanes is a simple, yet important issue, which had not been solved to date. Neutral rotaxanes had not been isolated because of their unusual stability; however, the

successful synthesis of free amine-type rotaxanes has now been achieved. The key to canceling this strong stabilization is the construction of a multiple equilibrium system and the successful removal of the conjugate acid from the reaction system (see scheme).

Rotaxanes

K. Nakazono, T. Takata* 13783–13794

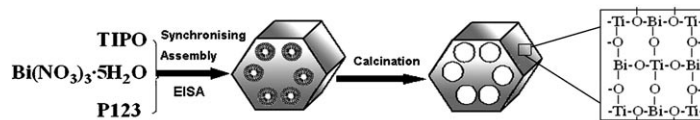
Neutralization of a *sec*-Ammonium Group Unusually Stabilized by the “Rotaxane Effect”: Synthesis, Structure, and Dynamic Nature of a “Free” *sec*-Amine/Crown Ether-Type Rotaxane



Mesoporous Materials

S. Sajjad, S. A. K. Leghari, F. Chen,
J. Zhang* 13795–13804

Bismuth-Doped Ordered Mesoporous TiO₂: Visible-Light Catalyst for Simultaneous Degradation of Phenol and Chromium



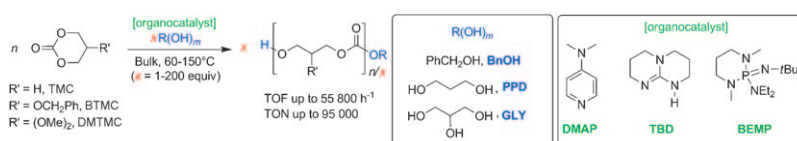
Bismuth cleans up: Highly ordered 2D hexagonal mesoporous (ms) crystalline Bi-doped TiO₂ nanocomposites that are active catalysts in the visible region have been synthesized (see figure). The photocatalytic activity of

2.0% Bi-doped ms-TiO₂ is far superior to other TiO₂ catalysts for the simultaneous degradation of phenol and reduction of chromium under visible illumination.

Ring-Opening Polymerization

M. Helou, O. Miserque, J.-M. Brusson,
J.-F. Carpentier,
S. M. Guillaume* 13805–13813

Organocatalysts for the Controlled “Immortal” Ring-Opening Polymerization of Six-Membered-Ring Cyclic Carbonates: A Metal-Free, Green Process



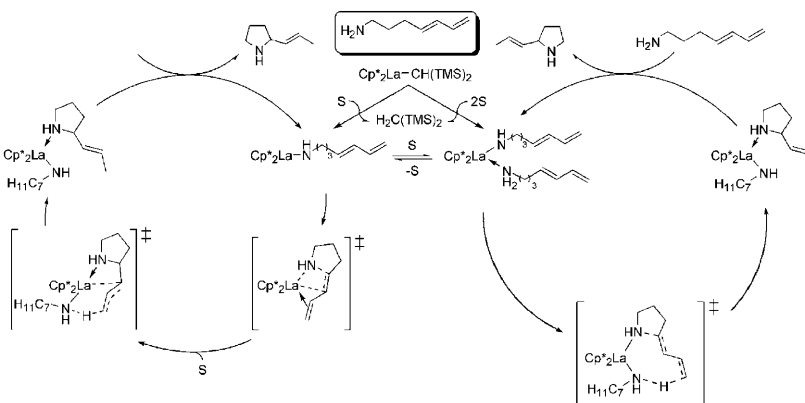
Show them the ROP(e)s! The organocatalyzed, “immortal” ring-opening polymerization of six-membered-ring carbonates has been evaluated on trimethylene carbonate (TMC) and its 3-substituted analogues DMTMC and BTMC (see scheme) by using a variety of organocatalysts, an amine (DMAP),

a guanidine (TBD), and a phosphazene (BEMP), in the presence of an alcohol (BnOH, PPD, or GLY), which acts both as a co-initiator and chain-transfer agent. The activities and productivities reached are among the highest reported for the ROP of cyclic carbonates.

Reaction Mechanisms

S. Tobisch* 13814–13824

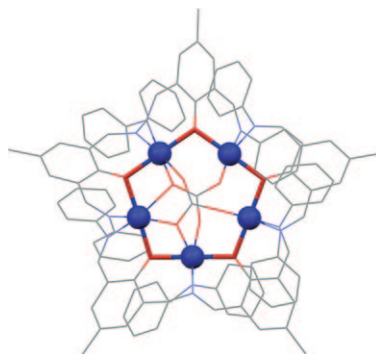
Mechanistic Investigation of Organolanthanide-Mediated Hydroamination of Conjugated Aminodienes: A Comprehensive Computational Assessment of Various Routes for Diene Activation



Rival routes for diene C=C activation in organolanthanide-catalysed hydroamination: Computational mechanistic analysis provides sound evidence of an operative Ln–N σ-bond insertive

mechanism with turnover-limiting aminolysis for intramolecular aminodiene hydroamination, whilst a non-insertive route is not achievable.

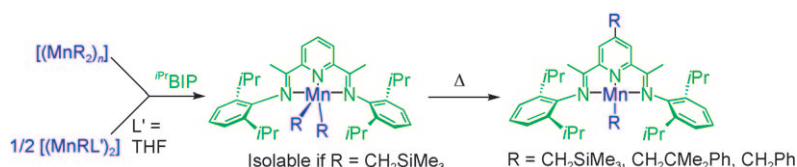
Facing spin-orbit coupling: A pentagonal $[\text{Co}^{\text{II}}_5]$ cluster has been synthesized, with the templating effect of CO_3^{2-} ions. The structure exhibits a topology of high-spin Co^{II} centers in a combination of geometries, which is suitable for testing a newly developed method to describe the spin-orbit coupling within polynuclear clusters of this ion.



Coordination Chemistry

M. Sarkar, G. Aromí, J. Cano,*
V. Bertolasi, D. Ray* 13825–13833*

Double- CO_3^{2-} Centered $[\text{Co}^{\text{II}}_5]$ Wheel and Modeling of Its Magnetic Properties



A (pre)cursor look at manganese chemistry: Dialkylmanganese(II) precursors provide a convenient entry to

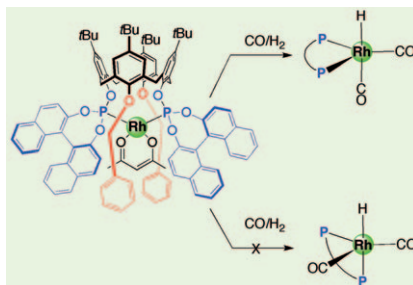
the organometallic chemistry of Mn complexes stabilised by 2,6-bisdiiminopyridine ligands (see scheme).

Coordination Chemistry

*C. M. Pérez, A. Rodríguez-Delgado,
P. Palma, E. Álvarez,
E. Gutiérrez-Puebla,
J. Cámpora* 13834–13842*

Neutral and Cationic Alkylmanganese(II) Complexes Containing 2,6-Bisiminopyridine Ligands

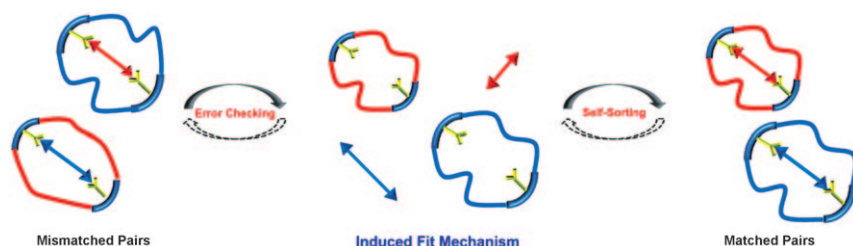
Rhodium in confinement: As revealed by high-pressure NMR/IR spectroscopic studies, the reaction of rhodium complexes containing hemispherical diphosphites with CO/H_2 leads to trigonal bipyramidal intermediates in which the phosphorus atoms exclusively occupy equatorial sites (see figure). The resulting metal confinement selectively drives olefin hydroformylation reactions to form aldehydes that best fit the cavity.



Homogeneous Catalysis

D. Sémeril, D. Matt,* L. Toupet,
W. Oberhauser,*
C. Bianchini 13843–13849*

High-Pressure Investigations under CO/H_2 of Rhodium Complexes Containing Hemispherical Diphosphites



All sorted out: A family of macrocycles composed of oligo(ethylene glycol) chains and diphenylbenzaldehyde residues was developed to construct a series of new incorporated

macrocycles through dynamic covalent chemistry. These flexible macrocycles exhibit excellent “self-sorting” abilities with diamines, in accordance with the “induced-fit” rule (see schematic).

Smart Molecules

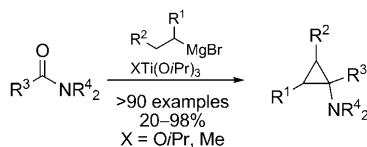
J.-M. Han, J.-L. Pan, T. Lei, C. Liu,
J. Pei* 13850–13861*

Smart Macrocyclic Molecules: Induced Fit and Ultrafast Self-Sorting Inclusion Behavior through Dynamic Covalent Chemistry



Organometallics

A. de Meijere,* V. Chaplinski,
H. Winsel, M. Kordes, B. Stecker,
V. Gazizova, A. I. Savchenko, R. Boese,
F. Schill (née Brackmann) 13862–13875



Ti is it: Cyclopropylamines have been obtained in low to excellent yield through the reaction of different *N,N*-dialkyl- and *N*-alkyl-*N*-phosphoryl-alkyl-substituted carboxamides with Grignard reagents in the presence of stoichiometric amounts of titanium tetraisopropoxide or methyltitanium triisopropoxide (see scheme).

Cyclopropylamines from *N,N*-Dialkylcarboxamides and Grignard Reagents in the Presence of Titanium Tetraisopropoxide or Methyltitanium Triisopropoxide

* Author to whom correspondence should be addressed

Supporting information on the WWW (see article for access details).

Full Papers labeled with this symbol have been judged by two referees as being “very important papers”.

A video clip is available as Supporting Information on the WWW (see article for access details).

SERVICE

Spotlights _____ 13568 Author Index _____ 13876 Keyword Index _____ 13877 Preview _____ 13879

Issue 45/2010 was published online on November 25, 2010

CORRIGENDUM

L. Zalewski,* M. Wykes, S. Brovelli,
M. Bonini, T. Breiner, M. Kastler,
F. Dötz, D. Beljonne,*
H. L. Anderson,* F. Cacialli,*
P. Samorì* 3933–3941

**A Conjugated Thiophene-Based
Rotaxane: Synthesis, Spectroscopy,
and Modeling**

Chem. Eur. J., **2010**, *16*

DOI: 10.1002/chem.200903353

There was an error in Figure 2 of the Full Paper. The assignment of the cyclodextrin protons marked at the top of Figure 2 is incorrect. The correct assignments are as follows: δ = 3.29 (dd, H2), 3.38 (t, H4), 3.43 (d, H6'), 3.57 (d, H5), 3.65 (d, H6), 3.72 ppm (t, H3). This error does not influence any other parts of the paper. We thank Christian Damblon (Liege) for pointing out this error.